Enhancing Electrocatalytic Activities of High-Entropy Borides (HEBs) for C–N Coupling in Induced Cation and pH-Dependent Microenvironments via Multiscale Modeling Strategy

Yan Feng[a], Yingchun Ding[b]; Li Liu[c,e*], Yi Xiao[d*].

[a]Xinjiang Vocational & Technical College of Communications, Urumqi, 831401, China.

[b]Department of Material and Chemical Engineering, Yibin University, Yibin Sichuan, 644000, China.

[c]Laboratory of New Energy and Materials, Xinjiang Institute of Engineering, Urumqi 830091, China.

[d]State Key Laboratory of Structural Chemistry, Chinese Academy of Sciences Fujian Institute of Research on the Structure of Matter, Fujian, Fuzhou 350002 (P. R. China).

[e]School of Chemistry and Chemical Engineering/State Key Laboratory Incubation Base for Green Processing of Chemical Engineering, Shihezi University, Shihezi 832003, China

Email addresses: 1643773723@qq.com (L. Liu)., xiaoyi@fjirsm.ac.cn (Y. Xiao).

Graphical abstract

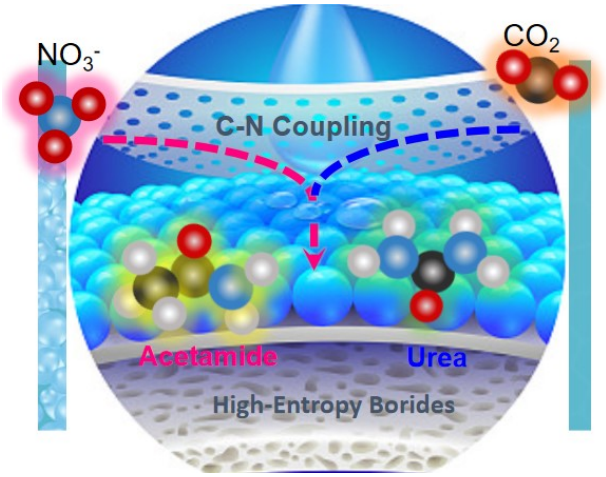

Mechanism pathway analysis

In this work, we proposed a new mechanism of the acetamide synthesis based on electrochemical Co-reduction of CO_2 and N_2 via C-N Coupling on high entropy alloy borides (HEA-MBene) materials.

(Acid environment)

1. CO_2 Reduction Reaction Pathway

1. $*+CO_2 \rightarrow *CO_2$
2. $*+CO_2+(H^++e^-) \rightarrow *COOH$
3. $*+CO_2+2(H^++e^-) \rightarrow *CO+H_2O$
4. $*+2CO_2+2(H^++e^-) \rightarrow *CO+*CO_2+H_2O$
5. $*+2CO_2+3(H^++e^-) \rightarrow *CO+*COOH+H_2O$
6. $*+2CO_2+4(H^++e^-) \rightarrow *CO*CO+2H_2O$
7. $*+2CO_2+5(H^++e^-) \rightarrow *COCOH+2H_2O$
8. $*+2CO_2+6(H^++e^-) \rightarrow *COHCOH+2H_2O$
9. $*+2CO_2+6(H^++e^-) \rightarrow *CCO+3H_2O$

2. **Amination Reaction Pathway**

1. $*+2CO_2+NH_3+6(H^++e^-) \rightarrow *CCOH(NH_2)+3H_2O$

2. $*+2CO_2+NH_3+6(H^++e-)\rightarrow *CHCO(NH_2)+3H_2O$

3. $*+2CO_2+NH_3+7(H^++e-)\rightarrow *CH_2CO(NH_2)+3H_2O$

4. $*+2CO_2+NH_3+8(H^++e-)\rightarrow *CH_3CO(NH_2)+3H_2O$

5. $*+2CO_2+NH_3+12(H^++e-)\rightarrow *CH_3CH_2NH_2+4H_2O$

3. Secondary Reaction

(COCO Path)

1. $*+CO_2+2(H^++e-)\rightarrow *CO+H_2O$

2. $*+2CO_2+3(H^++e-)\rightarrow *COCOOH+H_2O$

3. $*+2CO2+4(H^++e-)\rightarrow *CO*CO+2H_2O$

(COCOH Path)

1. $*+CO_2+3(H^++e-)\rightarrow *COH+H_2O$
2. $*+2CO_2+4(H++e-)\rightarrow *COHCOOH+H_2O$
3. $*+2CO_2+5(H++e-)\rightarrow *COHCO+2H_2O$

(CHOCO Path)

1. $*+CO_2+3(H^++e^-)\rightarrow *CHO+H_2O$
2. $*+2CO_2+4(H^++e^-)\rightarrow *CHOCOOH+H_2O$
3. $*+2CO_2+5(H^++e^-)\rightarrow *CHOCO+2H_2O$
4. $*+2CO_2+6(H^++e^-)\rightarrow *CH(OH)CO+2H_2O$

5. NO_3 Reduction Reaction Pathway

$*+NO_3+9(H^++e^-)\rightarrow *+NH_3+3H_2O$

1. $*NO_3\rightarrow *NO_3$
2. $*NO_3+(H^++e^-)\rightarrow *NOOOH$
3. $*NO_3+2(H^++e^-)\rightarrow *NO_2+H_2O$
3. $*NO_3+3(H^++e^-)\rightarrow *NOOH+H_2O$
4. $*NO_3+4(H^++e^-)\rightarrow *NO+2H_2O$
5. $*NO_3+5(H^++e^-)\rightarrow *NOH+2H_2O$
6. $*NO_3+6(H^++e^-)\rightarrow *N+3H_2O$
7. $*NO_3+7(H^++e^-)\rightarrow *NH+3H_2O$
8. $*NO_3+8(H^++e^-)\rightarrow *NH_2+3H_2O$
9. $*NO_3+9(H^++e^-)\rightarrow *NH_3+3H_2O$
10. $*NO_3+9(H^++e^-)\rightarrow *NH_3+3H_2O$
11. $*NO_3+9(H^++e^-)\rightarrow *+NH_3+3H_2O$
12. $*NO_3+5(H^++e^-)\rightarrow *HNO+2H_2O$
13. $*NO_3+6(H^++e^-)\rightarrow *HNOH+2H_2O$
14. $*NO_3+7(H^++e^-)\rightarrow *H_2NOH+2H_2O$

Urea synthesis

1. $*+CO_2\rightarrow *CO_2$

2. $*+CO_2+(H^++e^-)\rightarrow *COOH$

3. $*+CO_2+2(H^++e^-)\rightarrow *CO+H_2O$

4. $*+CO_2+H_2NOH+3(H^++e^-)\rightarrow *H_2NCO+2H_2O$

5. $*+CO_2+2H_2NOH+4(H^++e^-)\rightarrow *H_2NCONH_2+3H_2O$

(Alkaline environment)

Path CO_2RR (Alkaline)

1. $*+CO_2 \rightarrow *CO_2$

2. $*+CO_2+H_2O+2e^- \rightarrow *COOH+OH^-$

3. $*+CO_2+H_2O+2e^- \rightarrow *CO+2OH^-$

4. $*+2CO_2+2H_2O+4e^- \rightarrow *COCOOH+3OH^-$

5. $*+2CO_2+2H_2O+4e^- \rightarrow *COCO+4OH^-$

6. $*+2CO_2+3H_2O+6e^- \rightarrow *COCOH+5OH^-$

7. $*+2CO_2+4H_2O+8e^- \rightarrow *COHCOH+6OH^-$

8. $*+2CO_2+4H_2O+8e^- \rightarrow *CCO+6OH^-+H_2O$

9. $*+2CO_2+NH_3+4H_2O+8e^- \rightarrow *CC(OH)NH_2+6OH^-+H_2O$

10. $*+2CO_2+NH_3+4H_2O+8e^- \rightarrow *HCCONH_2+6OH^-+H_2O$

11. $*+2CO_2+NH_3+5H_2O+10e^- \rightarrow *H_2CCONH_2+7OH^-+H_2O$

12. $*+2CO_2+NH_3+6H_2O+12e^- \rightarrow *H_3CCONH_2+8OH^-+H_2O$

Path CHOCO (Alkaline)

4. $*+CO_2+2H_2O+4e^- \rightarrow *CHO+3OH^-$

5. $*+2CO_2+3H_2O+6e^- \rightarrow *CHOCOOH+4OH^-$

6. $*+2CO_2+3H_2O+6e^- \rightarrow *CHOCO+5OH^-$

7. $*+2CO_2+4H_2O+8e^- \rightarrow *HCOHCO+6OH^-$

Path COHCO (Alkaline)

4. $*+CO_2+2H_2O+4e^- \rightarrow *COH+3OH^-$

5. $*+2CO_2+3H_2O+6e^- \rightarrow *COHCOOH+4OH^-$

NO_3RR

Path A (Alkaline)

1. $*+NO_3 \rightarrow *NO_3$

2. $*+NO_3+H_2O+2e^- \rightarrow *NO_2+2OH^-$

3. $*+NO_3+2H_2O+4e^- \rightarrow *NO+4OH^-$

4. $*+NO_3+3H_2O+6e^- \rightarrow *N+6OH^-$

5. $*+NO_3+4H_2O+8e^- \rightarrow *NH+7OH^-$

6. $*+NO_3+5H_2O+10e^- \rightarrow *NH_2+8OH^-$

7. $*+NO_3+6H_2O+12e^- \rightarrow *NH_3+9OH^-$

8. $*+NO_3+6H_2O+12e^- \rightarrow *+NH_3+9OH^-$

Path B (Alkaline)

5. $*+NO_3+3H_2O+6e^- \rightarrow *NOH+5OH^-$

5. $*+NO_3+3H_2O+6e^- \rightarrow *HNO+5OH^-$

6. $*+NO_3+4H_2O+8e^- \rightarrow *HNOH+6OH^-$

7. $*+NO_3+5H_2O+10e^- \rightarrow *H_2NOH+7OH^-$

Urea synthesis

1. $*+CO_2+H_2NOH+H_2O+2e^- \rightarrow *H_2NCO+3OH^-$

2. $*+CO_2+2H_2NOH+H_2O+2e^- \rightarrow *H_2NCONH_2+4OH^-$

Computational hydrogen electrode model.

The energy of electron and proton pair is calculated as $1/2H_2$ according to calculated hydrogen

electrode (CHE) by Nørskov, which corresponds to reverse hydrogen electrode (RHE). Therefore, in the RHE, the chemical potential of a proton−electron pair was defined as $1/2H_2$. Therefore, in the RHE, the chemical potential of a proton-electron pair was defined as:

$$\Delta G(H^+ + e^-) = \frac{1}{2}\Delta G(H_2)$$

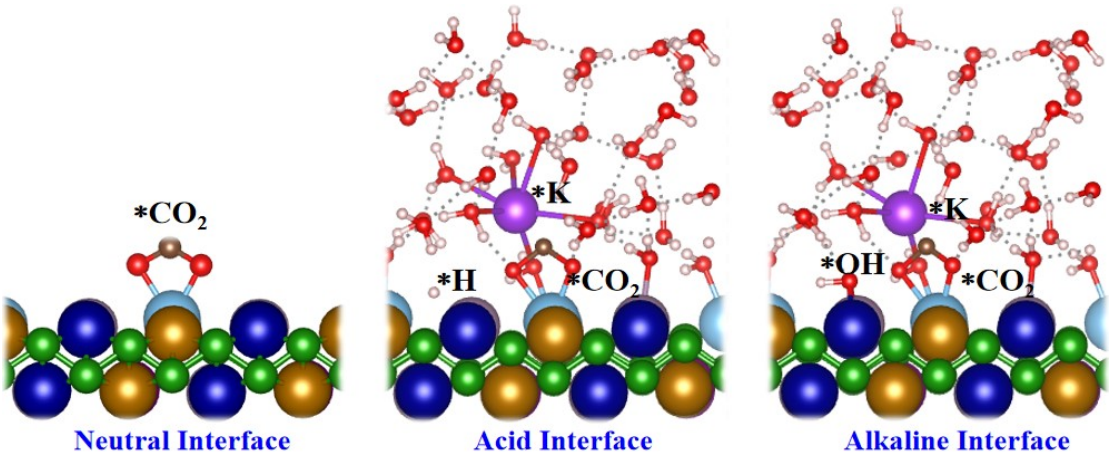

Computational model for neutral, acid and alkaline microenvironment interface.

Figures:

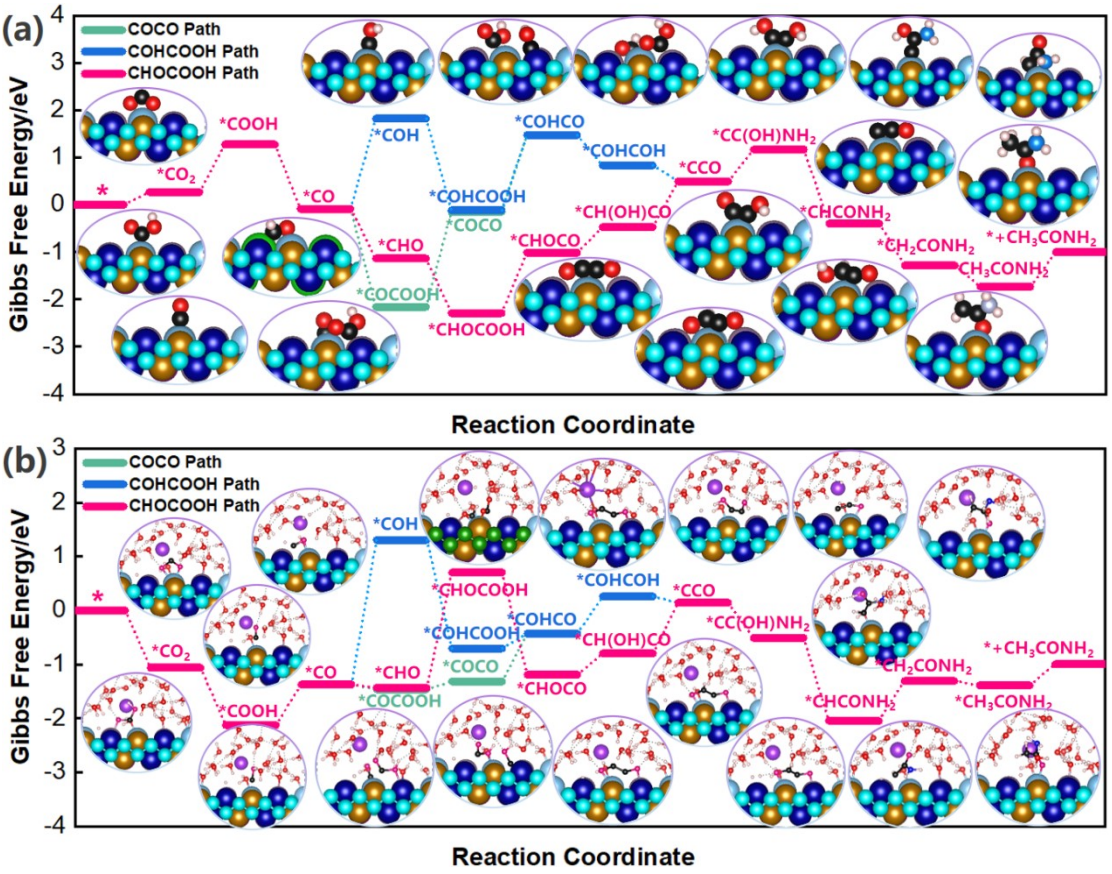

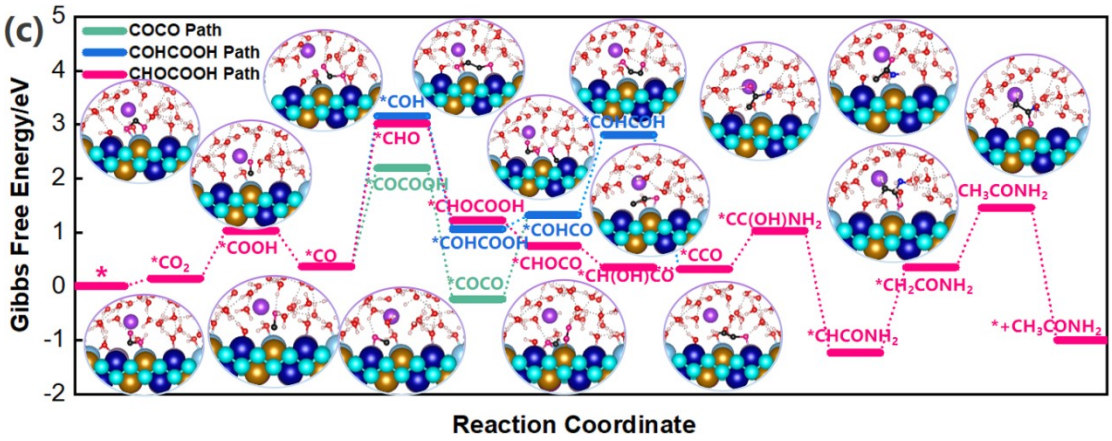

Figure S1. Calculated Gibbs free energy diagram via all potential energy profile path and corresponding their binding configurations of various intermediates generated over TiCrMnFeMoB (HEBs) catalysts during acetamide synthesis in (a) neutral, (b) acid and (c) alkaline environment, respectively.

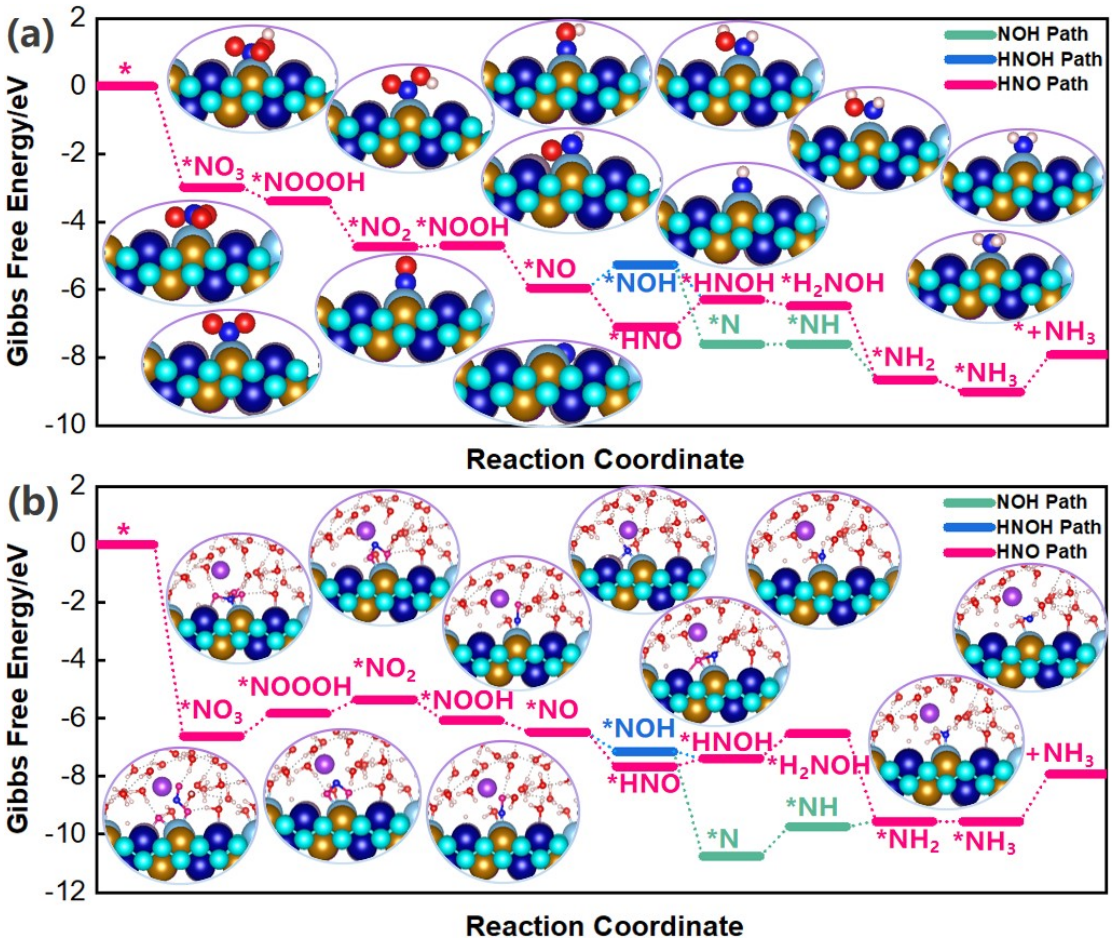

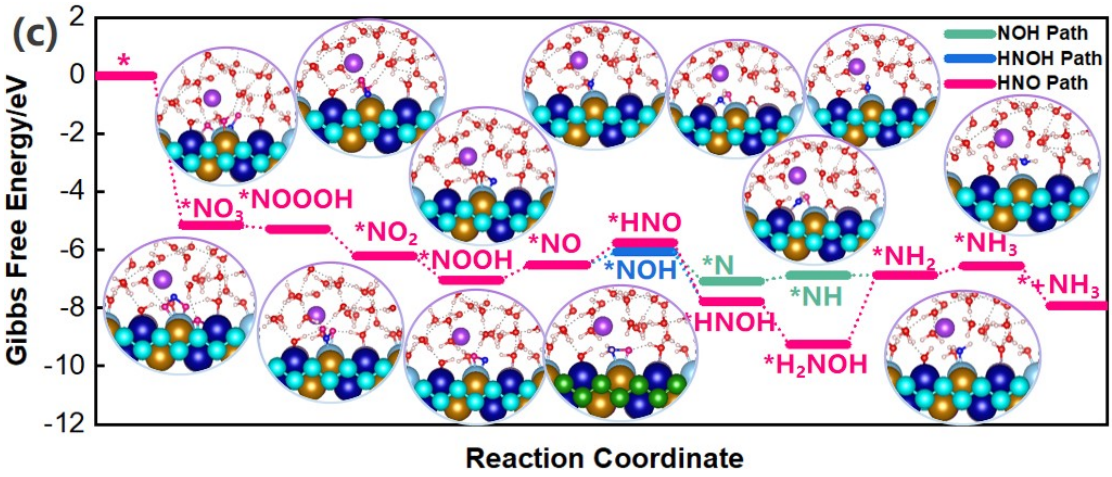

Figure S2. Calculated Gibbs free energy diagram via all potential energy profile path and corresponding their binding configurations of various intermediates generated over TiCrMnFeMoB (HEBs) catalysts during NH_3 and NH_2OH synthesis in (a) neutral, (b) acid and (c) alkaline environment, respectively.

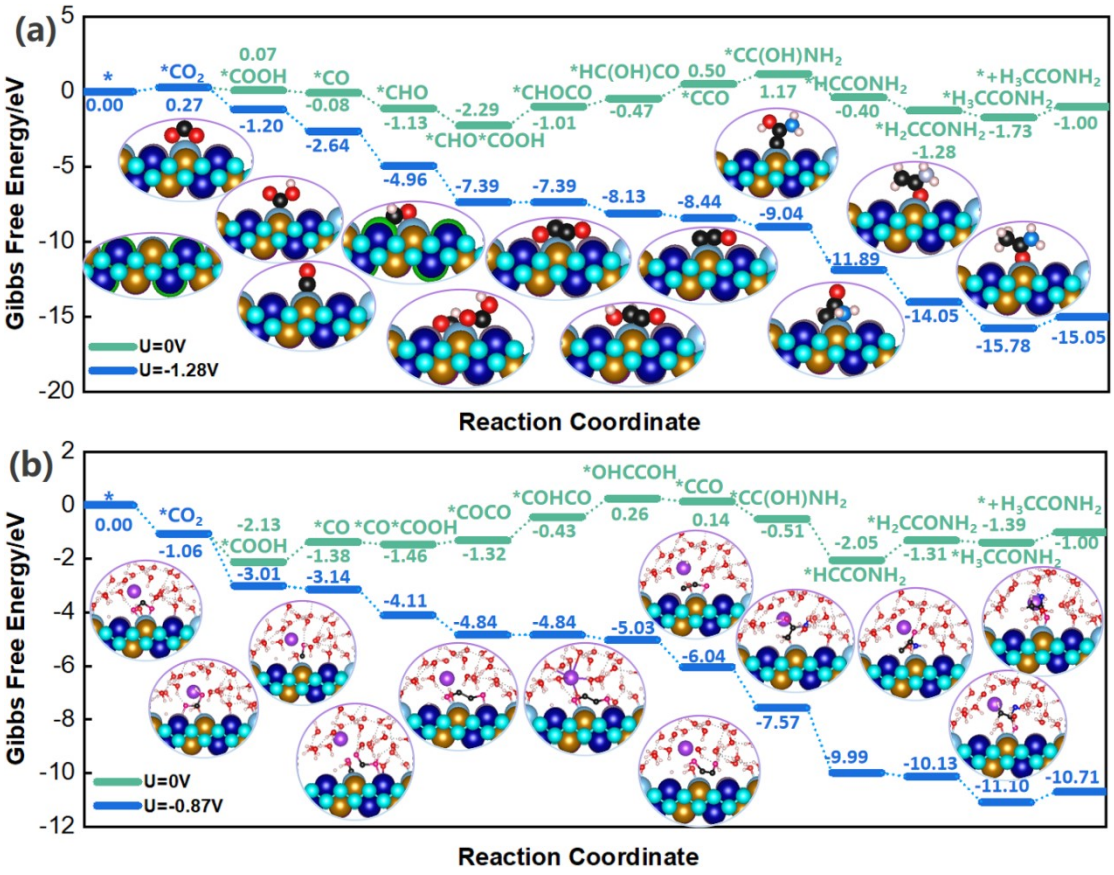

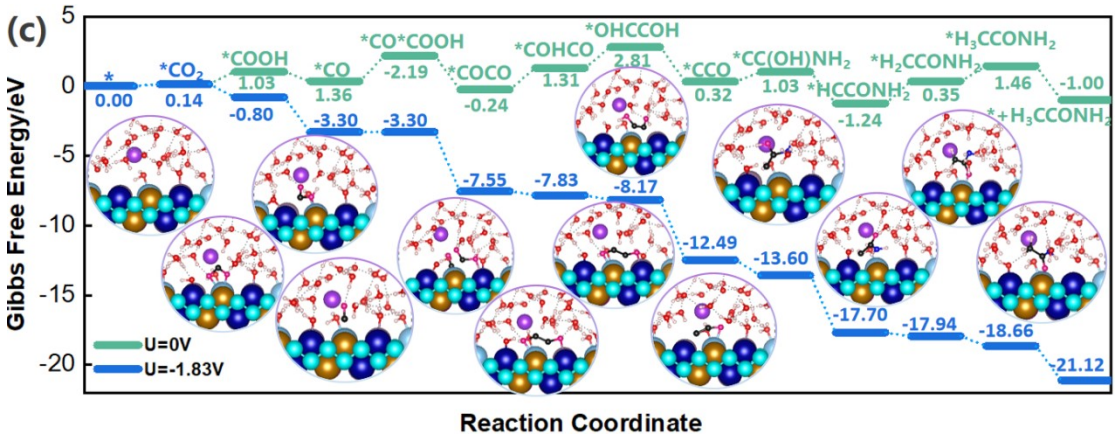

Figure S3. Calculated Gibbs free energy diagram under different applied potentials via the minimum energy profile path and corresponding binding configurations of various intermediates generated over TiCrMnFeMoB (HEBs) catalysts during acetamide synthesis in (a) neutral, (b) acid and (c) alkaline environment, respectively.

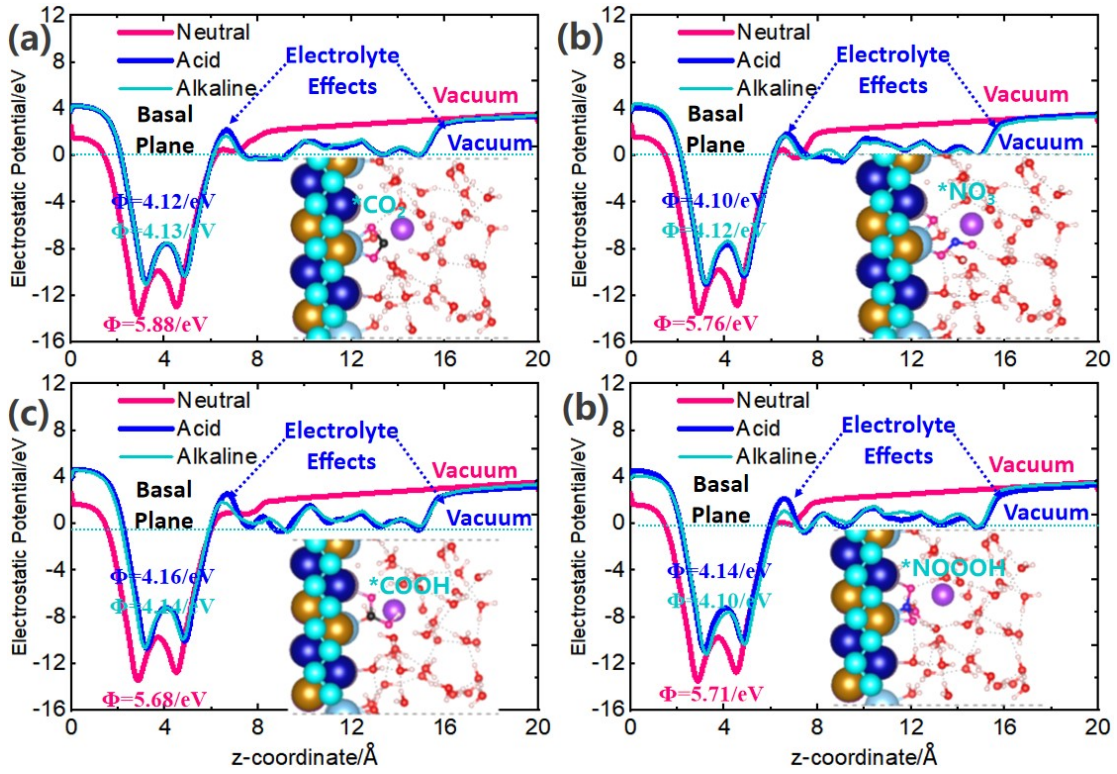

Figure S4. The electrostatic potential along z−direction slab model in neutral, acid and alkaline environments, a,c (Left) for CO2RR and b,d for NitrRR (Right) intermediates, respectively.

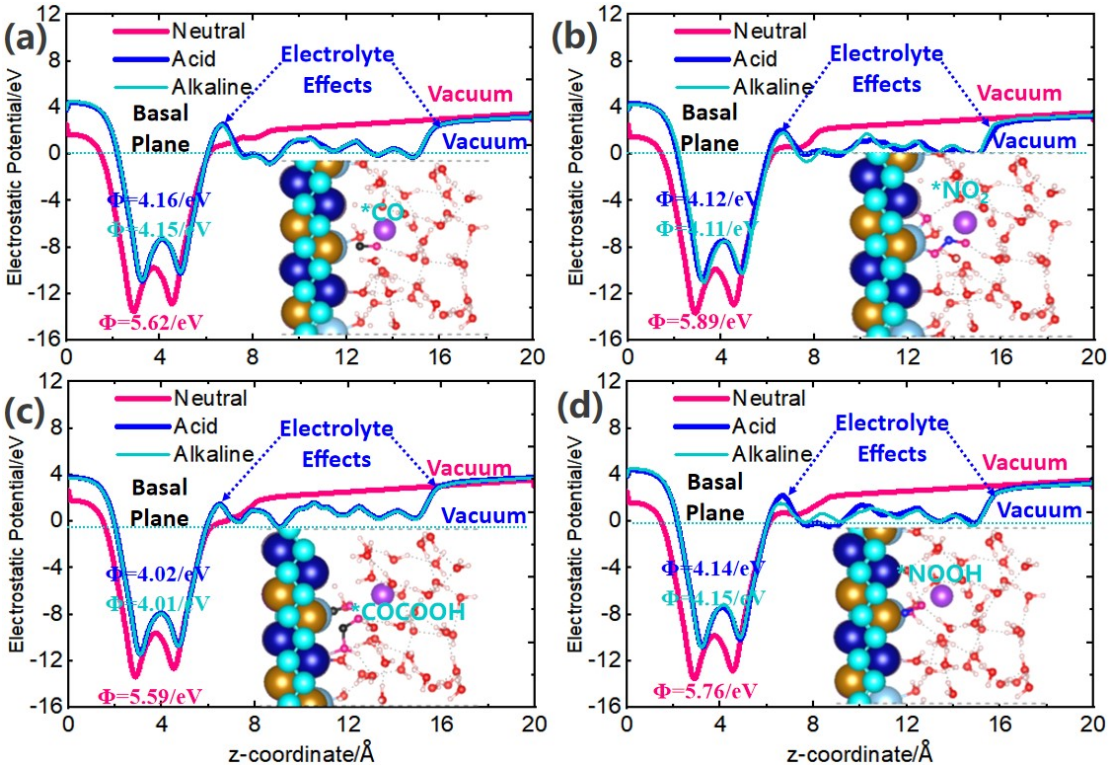

Figure S5. The electrostatic potential along z−direction slab model in neutral, acid and alkaline environments, a,c (Left) for CO2RR and b,d for NitrRR (Right) intermediates, respectively.

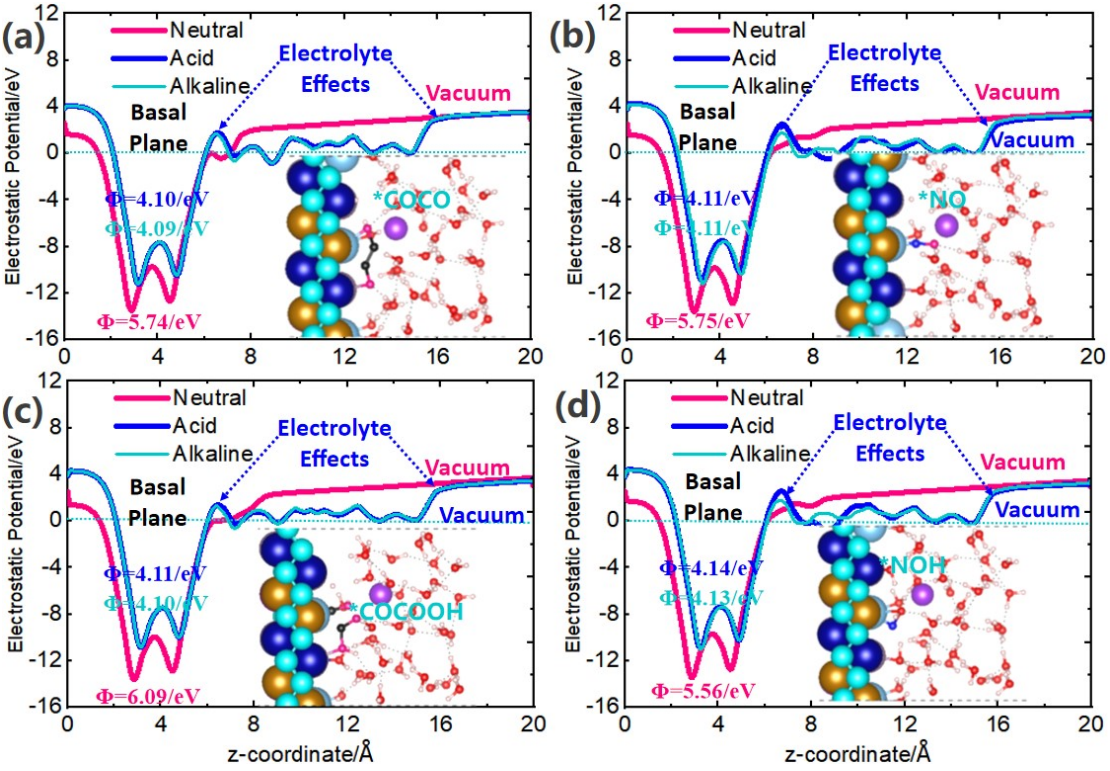

Figure S6. The electrostatic potential along z−direction slab model in neutral, acid and alkaline environments, a,c (Left) for CO2RR and b,d for NitrRR (Right) intermediates, respectively.

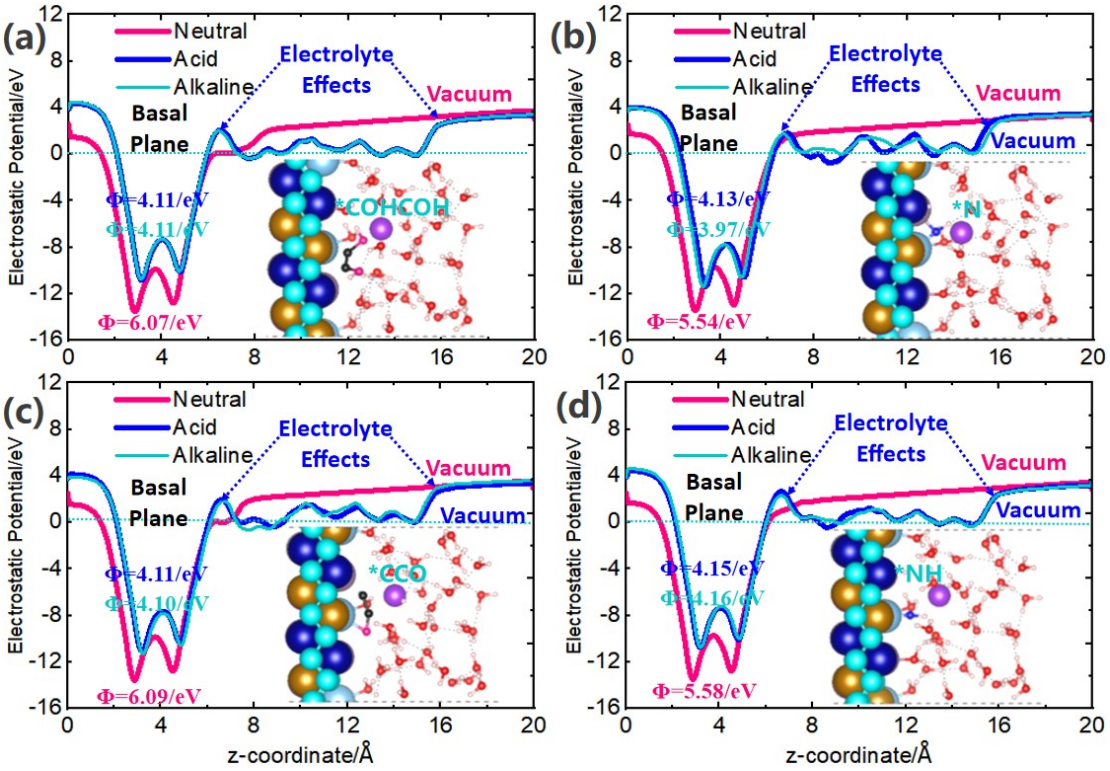

Figure S7. The electrostatic potential along z−direction slab model in neutral, acid and alkaline environments, a,c (Left) for CO2RR and b,d for NitrRR (Right) intermediates, respectively.

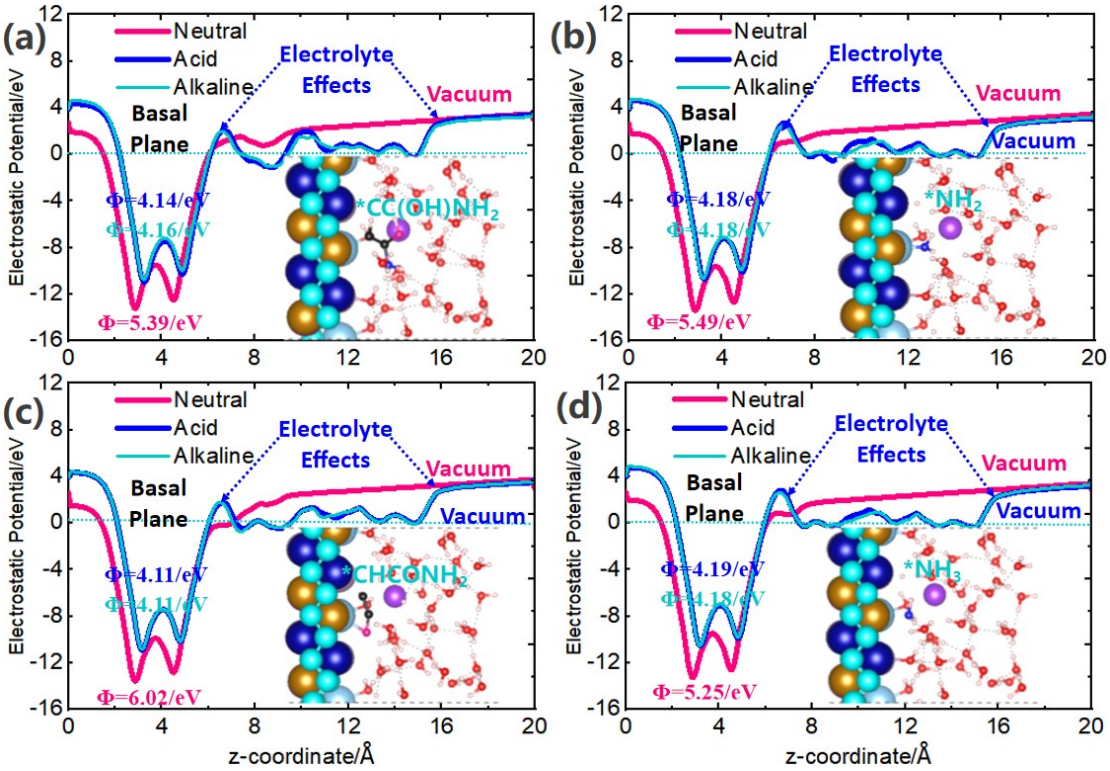

Figure S8. The electrostatic potential along z−direction slab model in neutral, acid and alkaline environments, a,c (Left) for CO2RR and b,d for NitrRR (Right) intermediates, respectively.

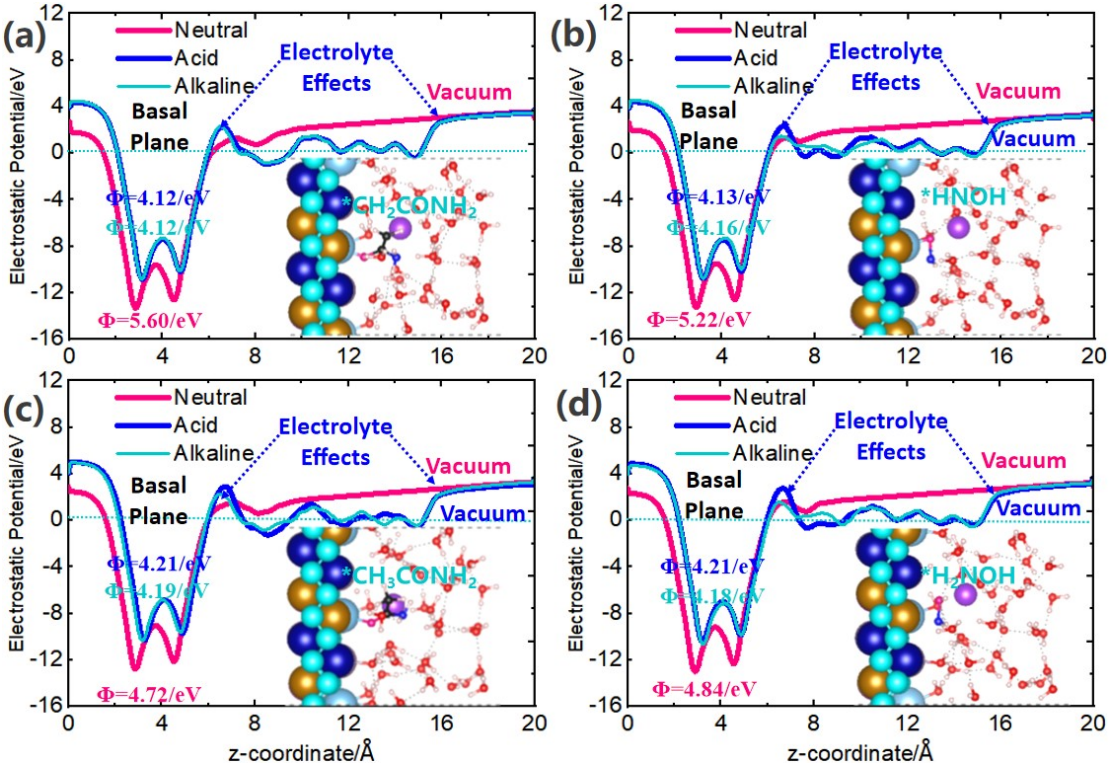

Figure S9. The electrostatic potential along z−direction slab model in neutral, acid and alkaline environments, a,c (Left) for CO2RR and b,d for NitrRR (Right) intermediates, respectively.

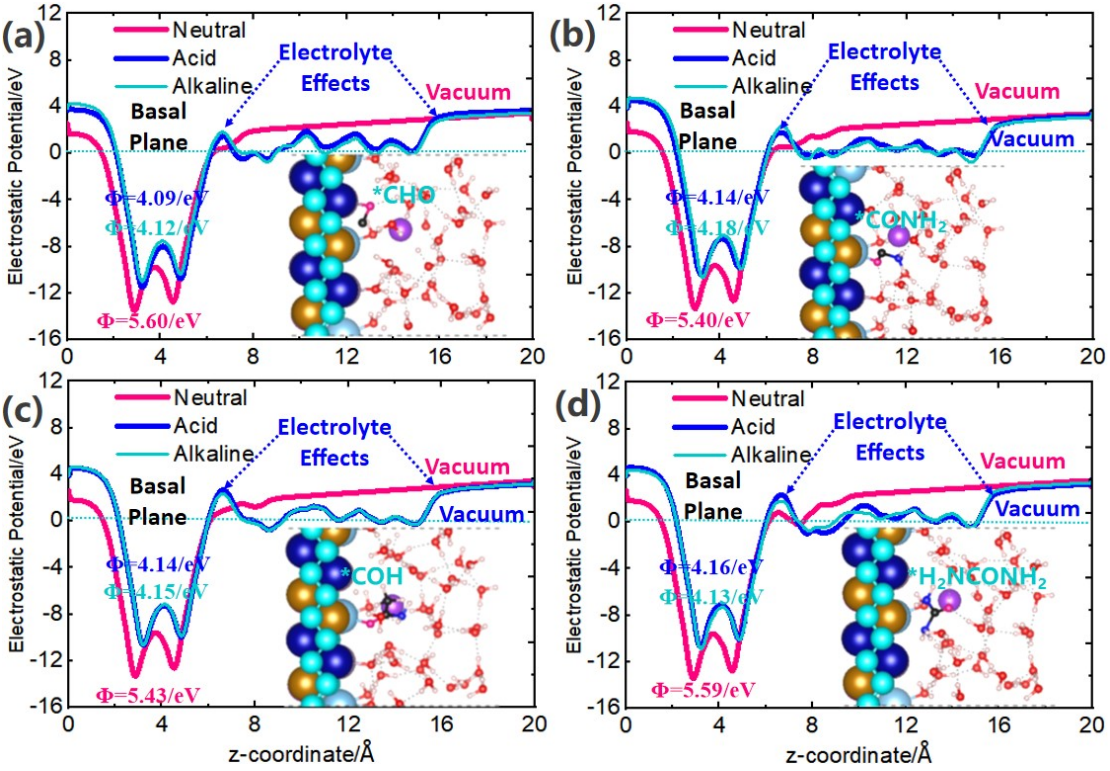

Figure S10. The electrostatic potential along z−direction slab model in neutral, acid and alkaline environments, a,c (Left) for CO2RR and b,d for NitrRR (Right) intermediates, respectively.

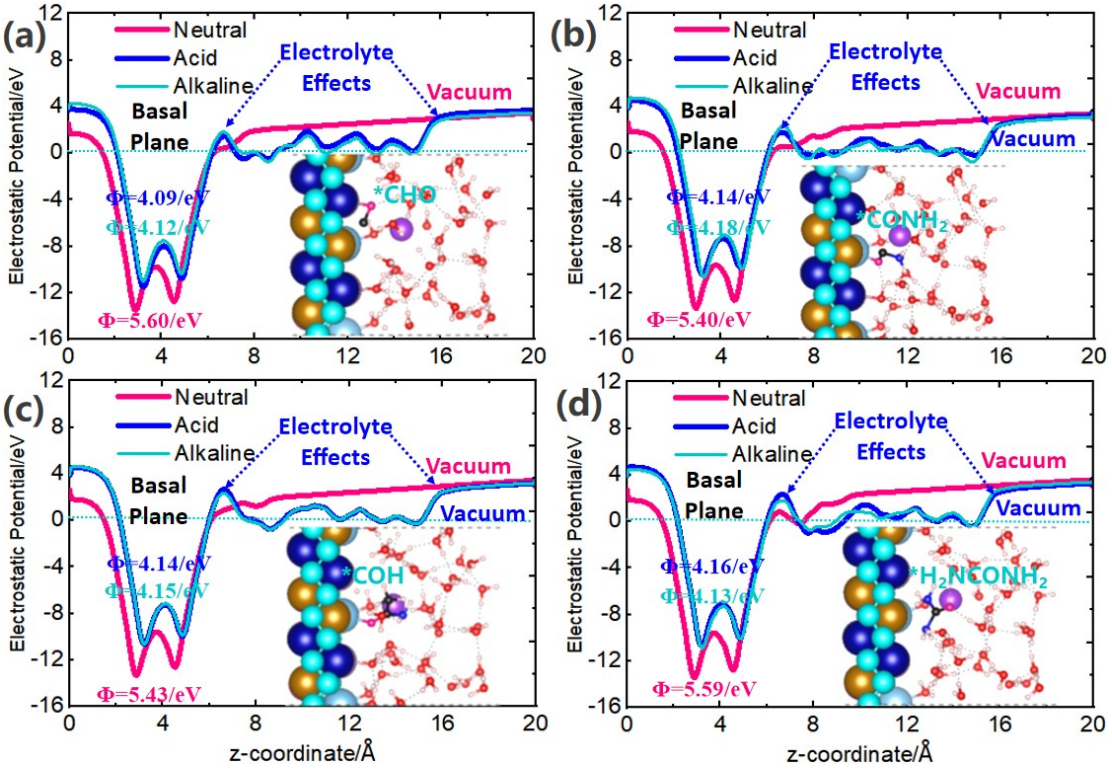

Figure S11. The electrostatic potential along z−direction slab model in neutral, acid and alkaline environments, a,c (Left) for CO2RR and b,d for NitrRR (Right) intermediates, respectively.

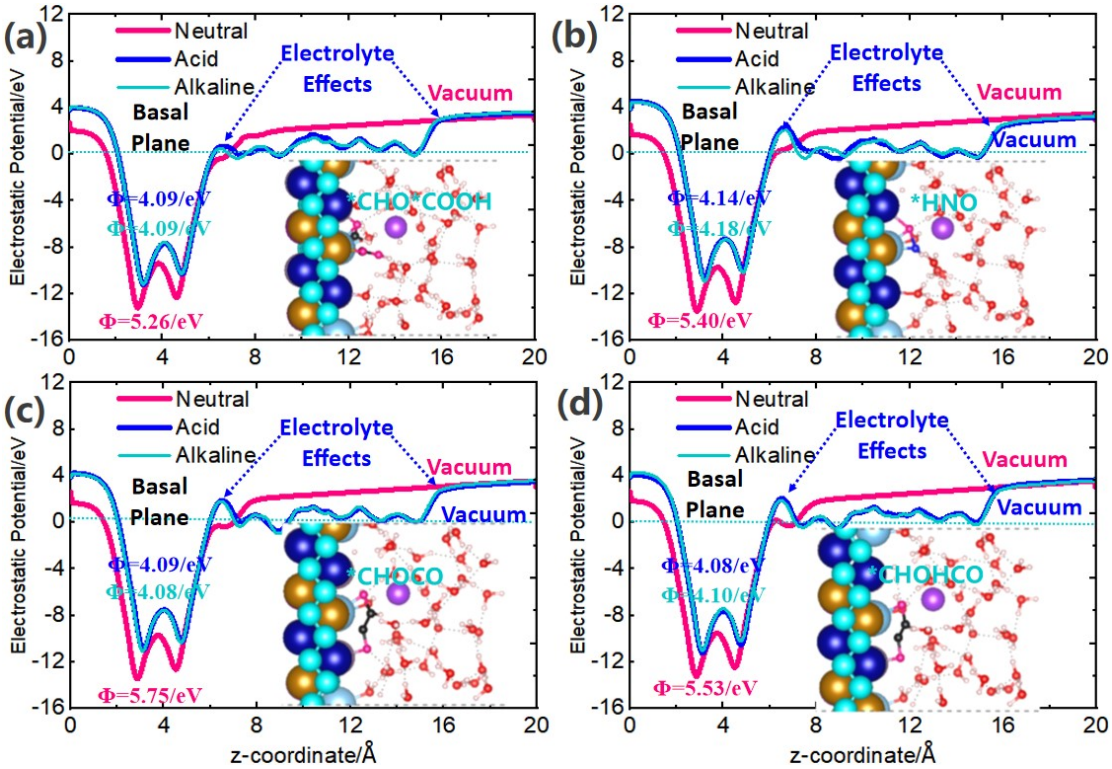

Figure S12. The electrostatic potential along z−direction slab model in neutral, acid and alkaline environments, a,c (Left) for CO2RR and b,d for NitrRR (Right) intermediates, respectively.

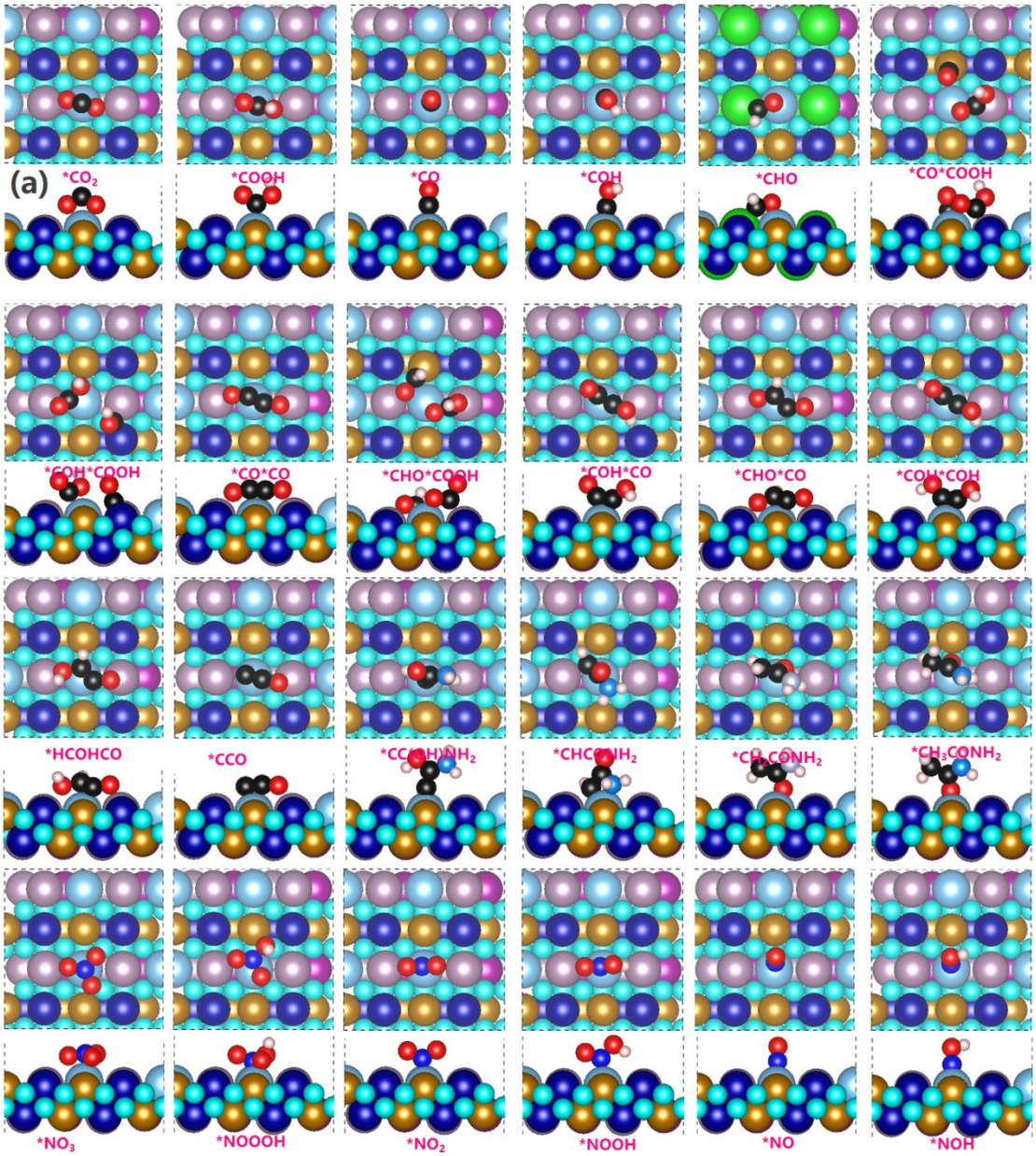
(a)
*CO2
*COOH
*CO
*COH
*CHO
*CO*COOH
*COH*COOH
*CO*CO
*CHO*COOH
*COH*CO
*CHO*CO
*COH*COH
*HCOHCO
*CCO
*CHCONH2
*CH2CONH2
*CH3CONH2
*NO3
*NOOOH
*NO2
*NOOH
*NO
*NOH

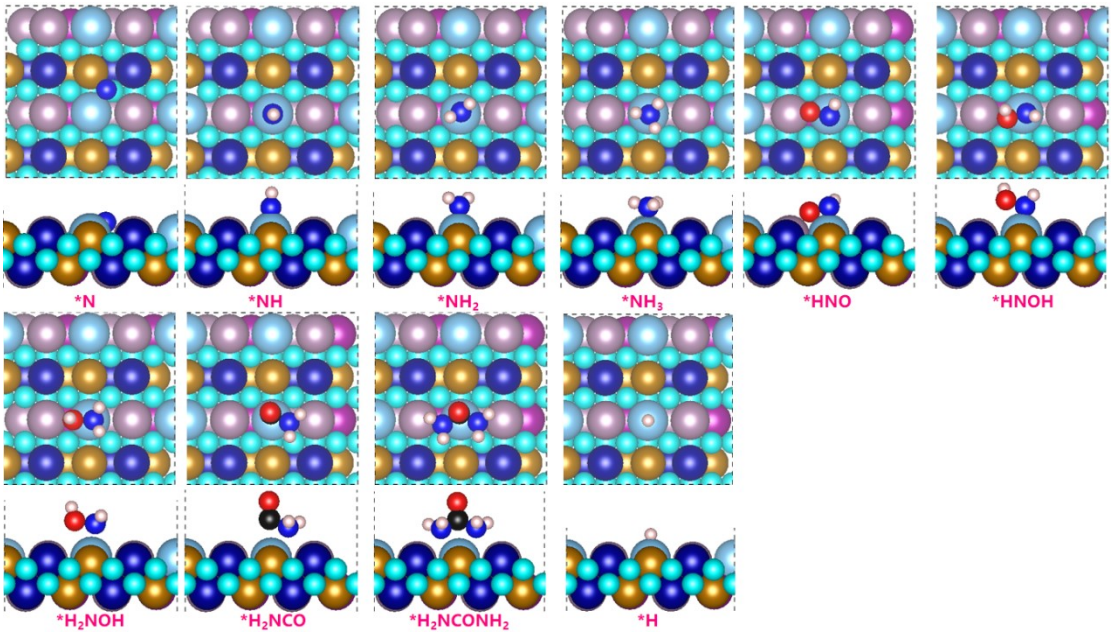

Figure S13. The corresponding binding configurations of various CO_2RR and NtrRR intermediates generated over TiCrMnFeMoB (HEBs) catalysts during acetamide synthesis in neutral environment.

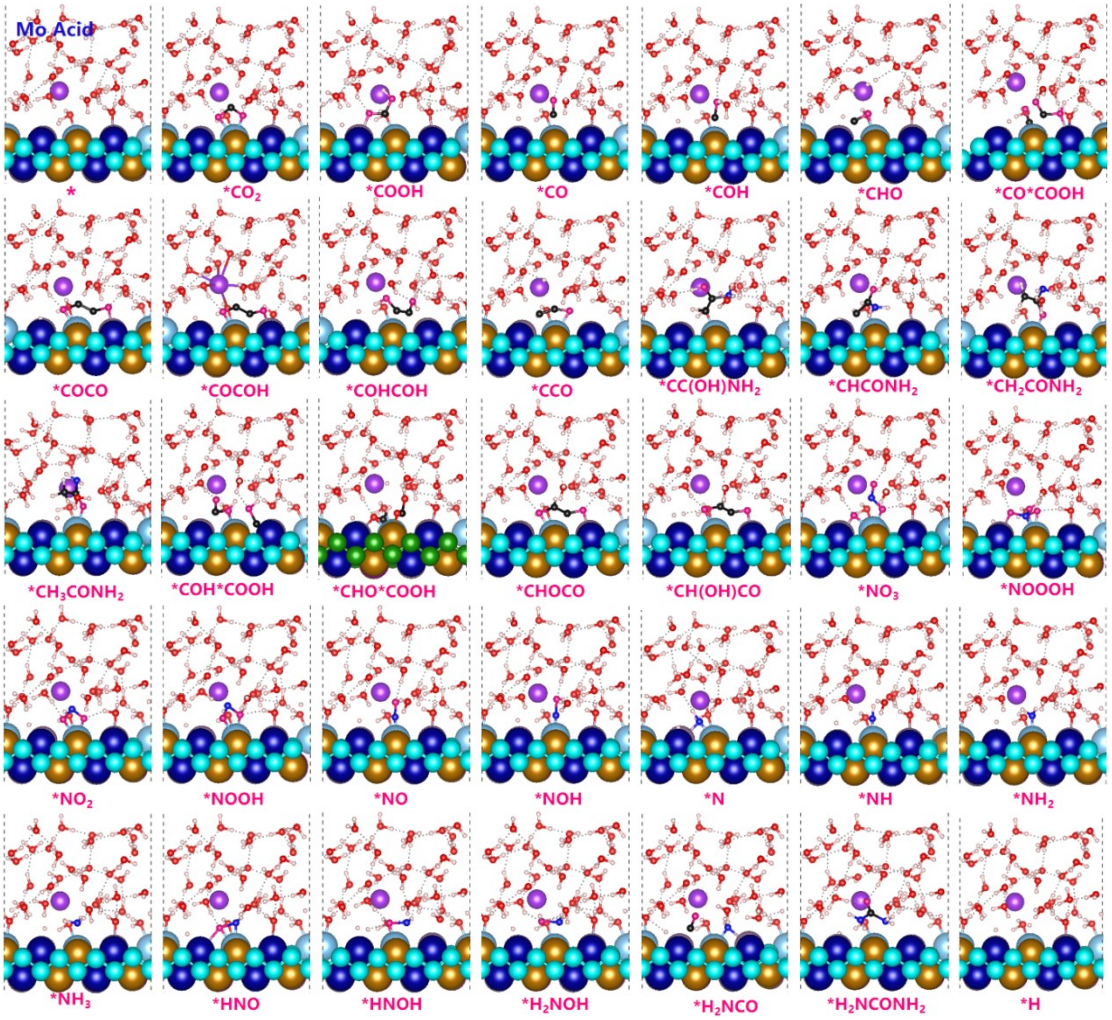

Figure S14. The corresponding binding configurations of various CO_2RR and NtrRR intermediates generated over TiCrMnFeMoB (HEBs) catalysts during acetamide synthesis in acid environment.

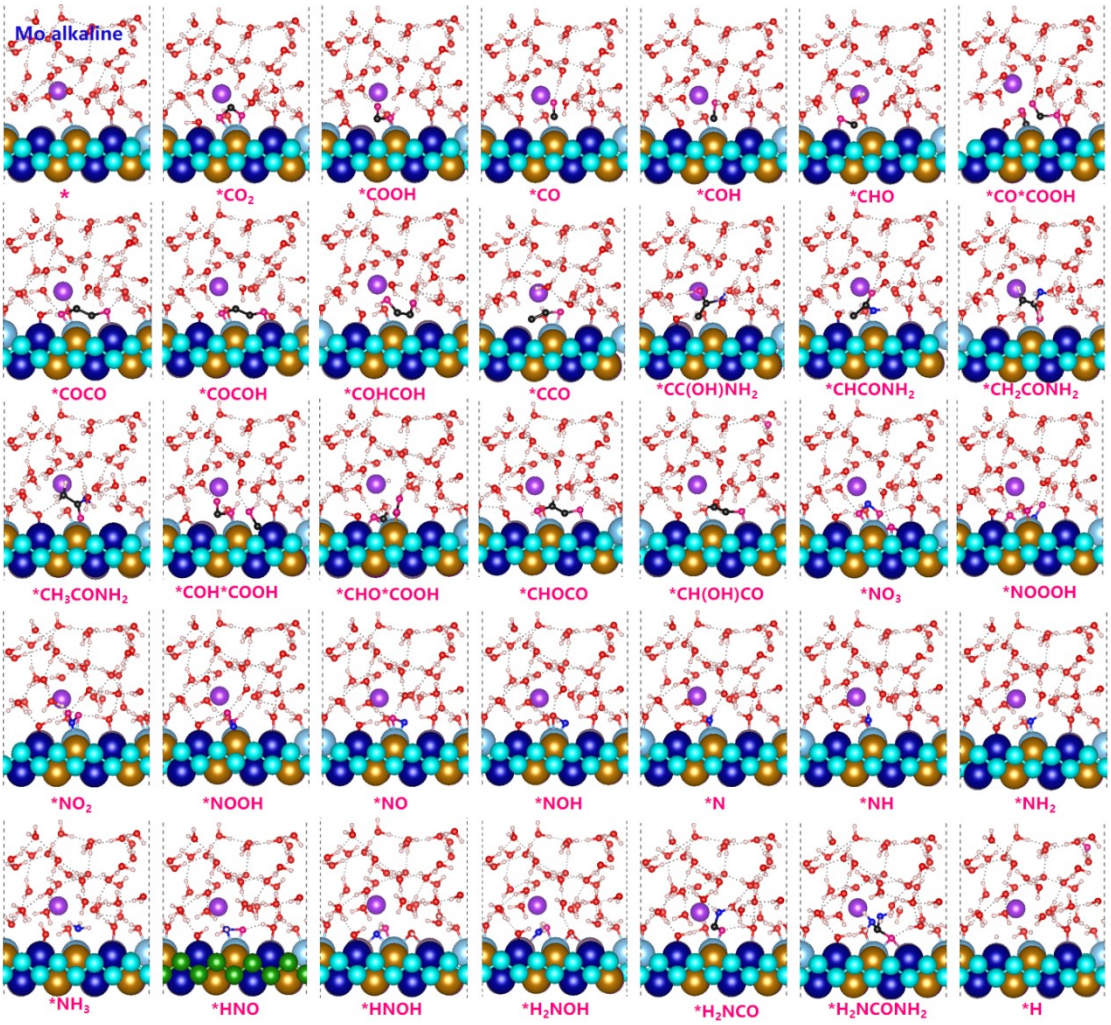

Figure S15. The corresponding binding configurations of various CO_2RR and NtrRR intermediates generated over TiCrMnFeMoB (HEBs) catalysts during acetamide synthesis in alkaline environment.

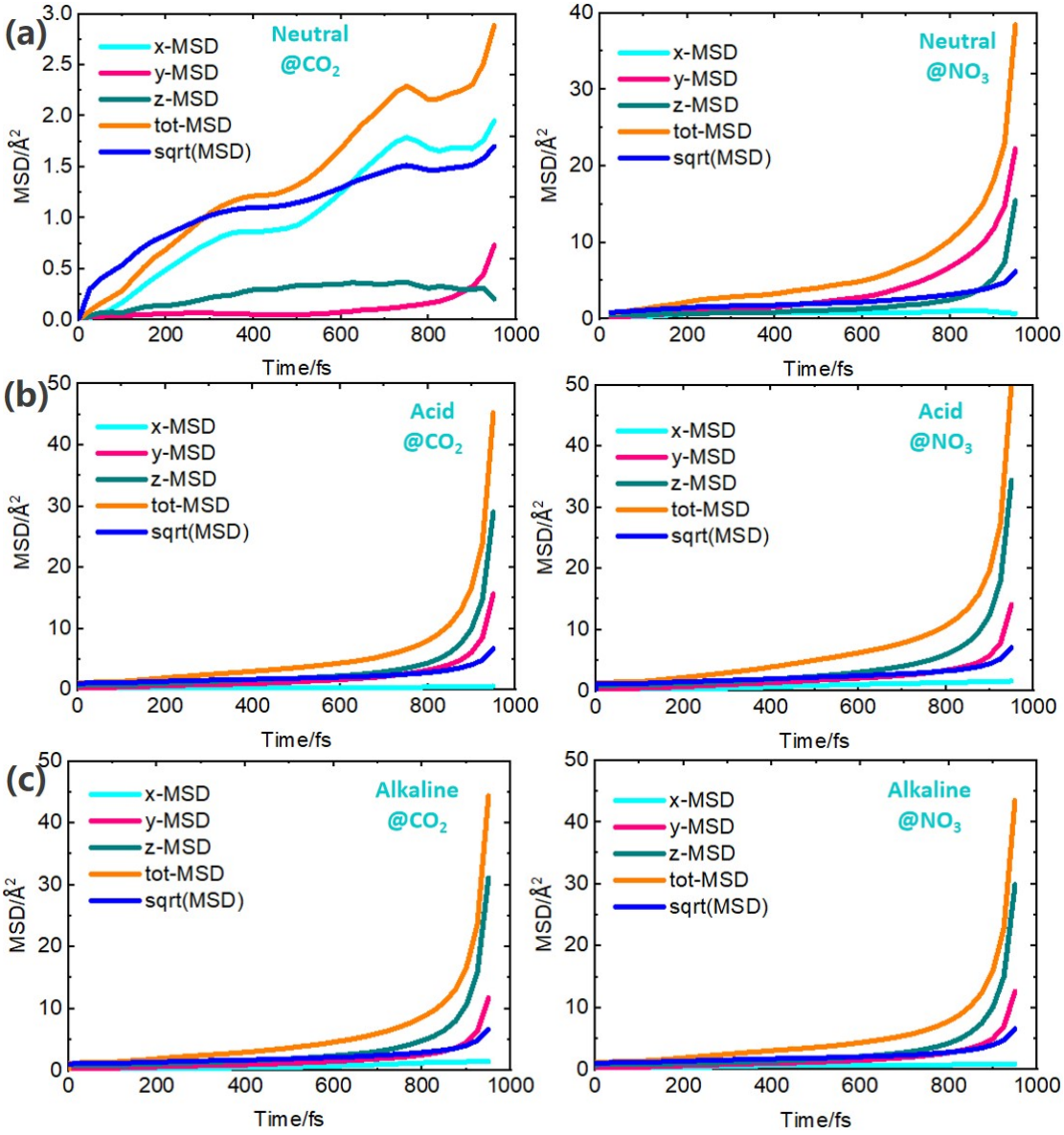

Figure S16. Time dependence of the mean square displacement (MSD) of the CO_2 (Left) and NO_3 (Right) adsorbed at neutral, acid and alkaline obtained by AIMD simulations, respectively.

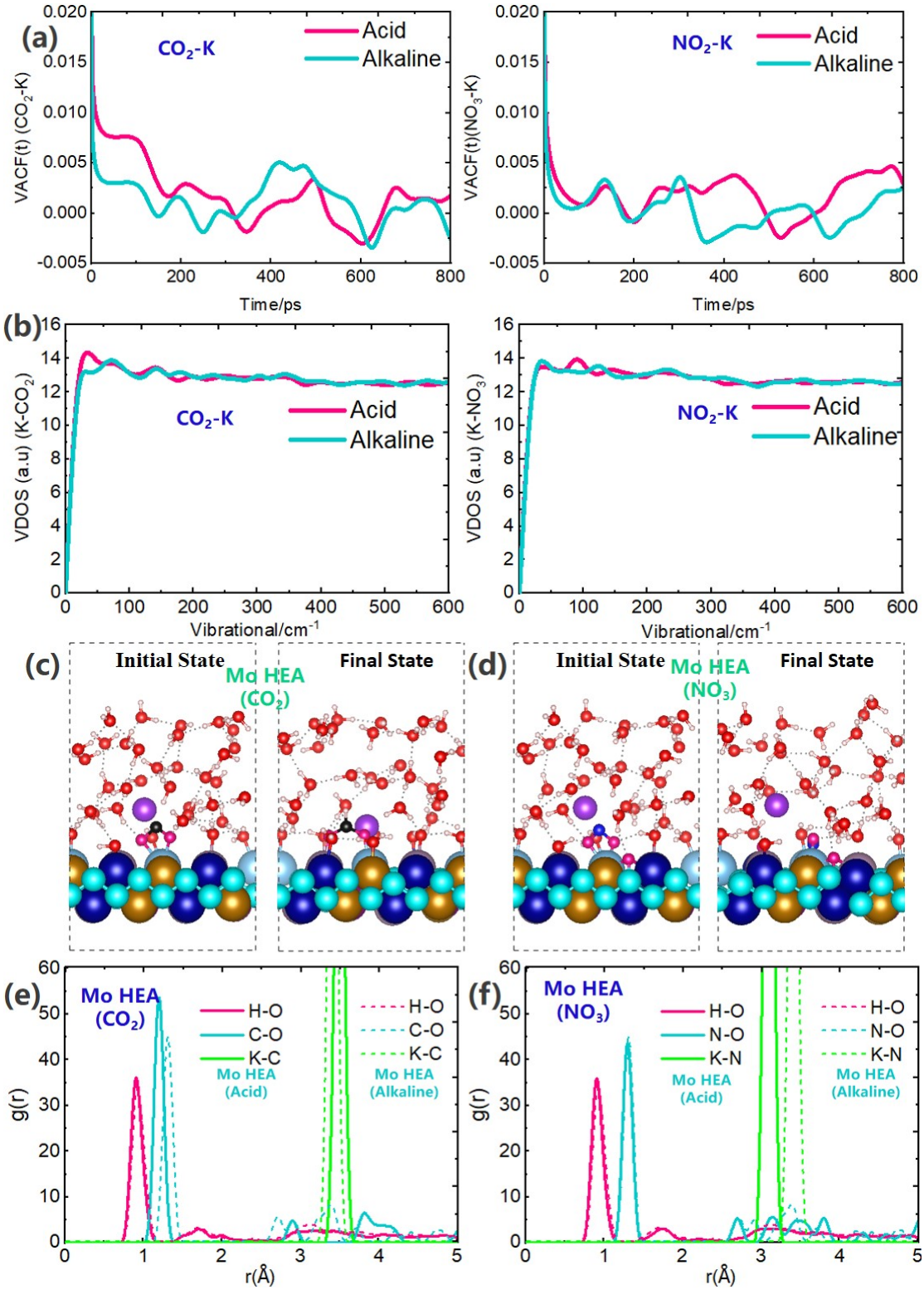

Figure S17. (a) The velocity autocorrelation function (VACF) of K+ cation in an aqueous acid solution over TiCrMnFeMoB (HEBs) catalysts for CO_2 (Left) and NO_3 (Right) adsorbed. (b) Vibrational density of states (VDOS) of K+ cation in an aqueous acid solution over TiCrMnFeMoB (HEBs) catalysts for CO_2 (Left) and NO_3 (Right) adsorbed. (c-d) AIMD snapshot of initial state and final state after 20ps simulation CO_2 (c) and NO_3 (d) adsorbed over TiCrMnFeMoB (HEBs) catalysts. (e-f) AIMD snapshot of radial distribution function (RDF) for O-H, C-O and K-C or K-N distance after 20ps simulation in CO_2 (e) and NO_3 (f) adsorbed over TiCrMnFeMoB (HEBs) catalysts, respectively.

Actually, in order to investigate the structural details involving in liquid–solid interface of the

CO_2RR to acetamide and urea, MD simulations were performed using a NVT ensemble at 300K. Fig 6c-d show the RDF between O atoms H atoms of cations HEB interface. The highest peak of RDF is relevant to O···H, and there is very low peak of RDF is relevant to O···H, which further confirms our previous conclusion that the CO_2 molecules prefer to attract with the K^+. In addition, the highest peak of RDF occurs at 1.0 Å, indicating the hydrogen bonds form between O atoms and H atoms with 1.7~1.3 Å distance. The peak is high involving in the strong interaction in H_3O^+ or OH^-, it also indicates that the role of water is the solvation when K^+ is added into the CO_2RR.

Fig 6e-f showed the RDF distribution of CO_2 molecules with K^+ cations in the near the HEB surface and number of the H-bond around one CO_2 molecule. Within the 5 Å distance from the center of a CO_2 molecule. Moreover, it can be seen from the structures that most of CO_2 molecules easily attach around the K^+ towards the C atom in CO_2 which is are consistent with our DFT results. Such structural distribution indicates the cation forms multi-ions synergistic catalytic mechanism by a mesoscale micro-environment, which will be elucidated in future work.

Table S1 The total Gibbs free energy of all CO_2RR and NtrRR intermediate species for acetamide and NH_3 or NH_2OH synthesis on TiCrMnFeMoB (HEBs) catalysts. * symbol represents the active states of intermediates.

System	Neutral	Acid	Alkaline	System	Neutral	Acid	Alkaline
Sur	-502.85	-1027.85	-1037.56	Sur	-502.85	-1027.85	-1037.56
*CO_2	-525.95	-1052.28	-1060.79	*NO_3	-529.14	-1057.78	-1066.03
*COOH	-528.38	-1056.78	-1063.34	*NOOOH	-532.99	-1060.44	-1069.60
*CO	-518.96	-1044.95	-1053.23	*NO_2	-523.56	-1049.18	-1059.75
*CO+*COOH	-547.83	-1072.14	-1078.20	*NOOH	-526.96	-1053.33	-1064.01
*COCO	-535.05	-1061.41	-1069.85	*NO	-517.44	-1042.95	-1052.72
*COCOH	-536.86	-1063.47	-1071.73	*NOH	-520.18	-1047.07	-1055.71
*COHCOH	-540.94	-1066.11	-1073.68	*N	-511.76	-1039.90	-1045.93
*CCO	-527.06	-1052.42	-1061.95	*NH	-515.18	-1042.31	-1049.18
*CC(OH)NH_2	-545.91	-1072.60	-1080.77	*NH_2	-519.67	-1045.57	-1052.59
*CHCONH_2	-547.48	-1074.43	-1083.04	*NH_3	-523.47	-1049.01	-1055.72
*CH_2CONH_2	-551.80	-1076.63	-1084.89	*HNO	-522.02	-1047.59	-1055.38
*CH_3CONH_2	-555.69	-1080.35	-1087.22	*HNOH	-524.65	-1050.74	-1060.85
*H	-506.03	-1031.69	-1041.69	*H_2NOH	-528.28	-1053.32	-1065.77
*COH	-520.49	-1046.01	-1053.87	*H_2NCO	-536.27	-1061.62	-1069.81
*CHO	-523.44	-1048.75	-1054.01	*H_2NCONH_2	-550.22	-1077.57	-1084.64
*COHCOOH	-549.23	-1074.82	-1082.77				
*CHOCOOH	-551.40	-1073.41	-1082.61				
*CHOCO	-539.35	-1064.53	-1072.30				
*CH(OH)CO	-542.24	-1067.57	-1076.14				

Table S2 The electrostatic potential, Fermi energy and work function of the charged system.

System	Vacuum	Work Function	E-fermi	System	Vacuum	Work Function	E-fermi	U_q(V/SHE) CO_2RR	U_q(V/SHE)NO_3RR
HEA	3.35	5.43	-2.09	HEA	3.35	5.43	-2.09	0.99	0.99
*CO_2	3.57	5.88	-2.30	*NO_3	3.56	5.76	-2.21	1.44	1.32
*COOH	3.53	5.68	-2.15	*NOOOH	3.54	5.71	-2.17	1.24	1.27

*CO	3.47	5.62	-2.15	*NO_2	3.56	5.89	-2.33	1.18	1.45
*CO*COOH	3.54	5.59	-2.05	*NOOH	3.53	5.76	-2.22	1.15	1.32
*COCO	3.56	5.74	-2.19	*NO	3.50	5.75	-2.25	1.30	1.31
*COCOH	3.69	6.09	-2.40	*NOH	3.45	5.56	-2.11	1.65	1.12
*COHCOH	3.74	6.07	-2.33	*N	3.41	5.54	-2.14	1.63	1.10
*CCO	3.55	5.83	-2.28	*NH	3.43	5.58	-2.16	1.39	1.14
*$CCOHNH_2$	3.46	5.39	-1.92	*NH_2	3.44	5.49	-2.05	0.95	1.05
*$CHCONH_2$	3.71	6.02	-2.32	*NH_3	3.37	5.25	-1.88	1.58	0.81
*CH_2CONH_2	3.58	5.60	-2.03	*HNO	3.48	5.65	-2.17	1.16	1.21
*CH_3CONH_2	3.29	4.72	-1.44	*HNOH	3.33	5.22	-1.89	0.28	0.78
CH_3CONH_2			0.00	*H_2NOH	3.23	4.84	-1.61		0.40
*H	3.40	5.63	-2.23					1.19	
*COH	3.42	5.43	-2.01	*H_2NCO	3.40	5.40	-2.01	0.99	0.96
*CHO	3.45	5.60	-2.15	*H_2NCONH_2	3.55	5.59	-2.04	1.16	1.15
*COHCOOH	3.47	5.45	-1.98	H_2NCONH_2				1.01	
*CHOCOOH	3.36	5.26	-1.90					0.82	
*CHOCO	3.57	5.75	-2.19					1.31	
*CH(OH)CO	3.54	5.53	-1.99					1.09	
HEA acid	4.60	4.17	0.44	HEA acid	4.60	4.17	0.44	-0.28	-0.28
*CO_2	4.25	4.12	0.13	*NO_3	4.11	4.10	0.02	-0.32	-0.34
*COOH	4.65	4.16	0.49	*NOOOH	4.56	4.14	0.41	-0.28	-0.30
*CO	4.45	4.14	0.31	*NO_2	4.36	4.12	0.24	-0.30	-0.32
*CO+*COOH	3.79	4.02	-0.23	*NOOH	4.42	4.14	0.28	-0.42	-0.30
*COCO	4.09	4.10	0.00	*NO	4.30	4.11	0.18	-0.35	-0.33
*COCOH	4.32	4.11	0.21	*NOH	4.42	4.14	0.28	-0.33	-0.30
*COHCOH	4.38	4.11	0.28	*N	4.01	4.13	-0.12	-0.33	-0.31
*CCO	4.14	4.11	0.03	*NH	4.45	4.15	0.30	-0.33	-0.29
*$CCOHNH_2$	4.35	4.14	0.21	*NH_2	4.62	4.18	0.44	-0.30	-0.27
*$CHCONH_2$	4.35	4.11	0.24	*NH_3	4.78	4.19	0.60	-0.33	-0.26
*CH_2CONH_2	4.39	4.12	0.28	*HNO	4.55	4.15	0.39	-0.33	-0.29
*CH_3CONH_2	5.02	4.21	0.81	*HNOH	4.42	4.13	0.29	-0.23	-0.31
CH_3CONH_2			0.00	*H_2NOH	4.88	4.21	0.67		-0.23
*H	4.48	4.17	0.31					-0.27	
*COH	4.56	4.14	0.42	*H_2NCO	4.55	4.14	0.41	-0.30	-0.30
*CHO	3.77	4.09	-0.32	*H_2NCONH_2	4.70	4.16	0.54	-0.35	-0.28
*COHCOOH	4.66	4.14	0.52	H_2NCONH_2				-0.30	
*CHOCOOH	4.00	4.09	-0.09					-0.35	
*CHOCO	4.22	4.09	0.13					-0.35	
*CH(OH)CO	4.09	4.08	0.00					-0.36	

HEA alkaline	4.25	4.14	0.11	HEA alkaline	4.25	4.14	0.11	-0.30	-0.30
*CO_2	4.26	4.13	0.14	*NO_3	4.43	4.12	0.32	-0.31	-0.32
*COOH	4.59	4.14	0.45	*NOOOH	4.13	4.11	0.02	-0.30	-0.33
*CO	4.54	4.15	0.39	*NO_2	4.27	4.11	0.16	-0.29	-0.33
*CO*COOH	3.54	5.59	-2.05	*NOOH	4.54	4.15	0.40	1.15	-0.30
*COCO	4.10	4.09	0.01	*NO	4.18	4.11	0.07	-0.35	-0.33
*COCOH	4.32	4.10	0.23	*NOH	4.40	4.13	0.27	-0.34	-0.31
*COHCOH	4.48	4.11	0.36	*N	4.10	3.97	0.13	-0.33	-0.47
*CCO	3.91	4.09	-0.17	*NH	4.61	4.16	0.45	-0.36	-0.28
*$CCOHNH_2$	4.63	4.16	0.48	*NH_2	4.74	4.18	0.56	-0.28	-0.26
*$CHCONH_2$	4.40	4.11	0.30	*NH_3	4.88	4.18	0.70	-0.33	-0.26
*CH_2CONH_2	4.49	4.12	0.36	*HNO	4.47	4.14	0.33	-0.32	-0.30
*CH_3CONH_2	4.98	4.19	0.80	*HNOH	4.55	4.16	0.39	-0.26	-0.29
CH_3CONH_2			0.00	*H_2NOH	4.72	4.18	0.53		-0.26
*H	4.48	4.17	0.31					-0.27	
*COH	4.64	4.15	0.49	*H_2NCO	4.78	4.18	0.60	-0.30	-0.26
*CHO	4.26	4.12	0.15	*H_2NCO NH_2	4.46	4.13	0.33	-0.32	-0.31
*COHCOOH	4.60	4.12	0.49	H_2NCON H_2				-0.32	
*CHOCOOH	4.05	4.09	-0.04					-0.36	
*CHOCO	4.16	4.08	0.08					-0.36	
*CH(OH)CO	4.30	4.10	0.20					-0.34	

Table S3 the Gibbs free energy of the gas molecular from the DFT calculation at 298.15 K (T).

CO_2	-23.36583388	H_2	-6.87426486	CH_3CONH_2	-52.10930419	NO_3	-23.31657567
NH_3	-19.52793996	H_2O	-14.21570483	NH_2CONH_2	-46.49885425	*H_2NOH	-24.47159266

Table S4. Comparison of the CO2RR performance of high-entropy alloy catalytic systems.

Reaction	Potential barrier	High-entropy alloy	Reaction	Potential barrier	High-entropy alloy
CO2RR	1.996	AgScTiWZn	NRR	0.634	HfLaPbVZn
	2.041	AlInScTlY		0.639	CdLaPbTaV
	2.057	CrNbPbZnZr		0.672	NbPbRhTiY
	2.062	AuScTiVY		0.677	AuGaHfSnY
	2.076	CoHfHgScTi		0.678	CrReSnWZr
	2.084	AgAuFeHfLa		0.678	AlCrPbTiW
	2.094	HfPbScTiTl		0.687	AgHfPbScTl
	2.1	IrScTaTcTl		0.689	IrLaTaWY
	2.105	CdHfMoNbZn		0.692	BiPbScTiZr
	2.11	AlCdHfTaW		0.702	BiMnNiSnTl

Table S5. Summary of synthesis methods for HEAs electrocatalysts.

Catalyst	Structure	Synthetic method	Catalytic reaction	Ref.
PtPdRhNi and PtPdFeCoNi	FCC	Carbothermal shock	ORR	[1]
RuIrCeNi and RuIrCeNiWCuCrCo	FCC	Carbothermal shock	ORR and OER	[2]
PtNiFeCoCu	FCC	Colloidal synthesis	HER and MOR	[3]
PdFeCoNiCu	BCC	Colloidal synthesis	HER	[4]
RuFeCoNiCu	HCP	Colloidal synthesis	NRR	[5]
PdCuPtNiCo	FCC	Colloidal synthesis	ORR	[6]
MnFeCoNiCu	FCC	Solvothermal	OER	[7]
IrPdPtRhRu	FCC	Polyol method	HER	[8]
IrOsPdPtRhRu	FCC	Polyol method	EOR	[9]
IrOsReRhRu	HCP	Thermal decomposition	MOR	[0]
CoFeLaNiPt	Amorphous	Electrodeposition	OER and HER	[11]
FeCoPdIrPt	FCC	Fast moving bed pyrolysis	HER	[12]
AlNiCoIrMo	FCC	Dealloying	OER	[13]
AlNiCoFeX (X = Mo, Nb, and Cr)	FCC	Dealloying	OER	[14]
AlNiCoFeX (X = Mo, Nb, and Cr)	FCC	Dealloying	ORR and OER	[15]

The activity of a catalyst generally depends on its specific sur- face area, because larger surface areas expose more reactive sites. However, the current HEA fabrication methods (e.g., mechanical alloying, arc melting, magnetron sputtering, laser deposition, etc.) tend to produce bulk mate- rials. Therefore, to reduce the sizes of HEAs and increase their specific surface areas, it is imperative to develop new synthetic methods for HEA preparation (Table).

Table S6 the adsorption energy and Bader charge transfer of the CO_2 and NO_3^- molecular from the DFT calculation.

Systems	Neutral		Acid		Alkaline	
	E_{ads}	Bader Charge	E_{ads}	Bader Charge	E_{ads}	Bader Charge
CO_2	0.26958	0.738875	−1.06318	1.043732	0.14239	0.959345
NO_3^-	−2.97533	1.06417	−6.61591	0.090739	−5.14707	2.20659

Table S7 Total energies (E_{tot}) of $*CO_2$ and $*NO_3$ on HEB surfaces at different potentials (vs reversible hydrogen electrode).

U_{SHE}	-2	-1.5	-1	-0.5	0	0.5	1	1.5	2
Neutral	-507.03	-505.98	-504.94	-503.89	-502.85	-501.81	-500.76	-499.72	-498.67
*CO2	-530.55	-529.4	-528.25	-527.1	-525.95	-524.79	-523.64	-522.49	-521.34
Acid	-1026.98	-1027.2	-1027.41	-1027.63	-1027.85	-1028.07	-1028.29	-1028.51	-1028.72
*CO2	-1052.02	-1052.08	-1052.15	-1052.21	-1052.28	-1052.35	-1052.41	-1052.48	-1052.54
Alkaline	-1036.69	-1036.91	-1037.13	-1037.35	-1037.56	-1037.78	-1038	-1038.22	-1038.44
*CO2	-1060.53	-1060.59	-1060.66	-1060.72	-1060.79	-1060.85	-1060.92	-1060.98	-1061.05
Neutral	-507.03	-505.98	-504.94	-503.89	-502.85	-501.81	-500.76	-499.72	-498.67
*NO3	-533.55	-532.45	-531.35	-530.24	-529.14	-528.04	-526.94	-525.83	-524.73

Acid	-1026.98	-1027.2	-1027.41	-1027.63	-1027.85	-1028.07	-1028.29	-1028.51	-1028.72
*NO3	-1057.75	-1057.76	-1057.77	-1057.78	-1057.78	-1057.79	-1057.8	-1057.81	-1057.82
Mo alkaline	-1037.35	-1037.4	-1037.46	-1037.51	-1037.56	-1037.62	-1037.67	-1037.72	-1037.78
*NO3	-1065.4	-1065.55	-1065.71	-1065.87	-1066.03	-1066.18	-1066.34	-1066.5	-1066.66

Table S8 Binding energies of $*CO_2$ and $*NO_3$ on HEB surfaces at different potentials (vs reversible hydrogen electrode).

Applied Potential	-2.00	-1.50	-1.00	-0.50	0.00	0.50	1.00	1.50	2.00
U_{SHE}	-0.16	-0.05	0.05	0.16	0.27	0.38	0.48	0.59	0.7
Acid $*CO_2$	-1.68	-1.52	-1.37	-1.22	-1.06	-0.91	-0.76	-0.6	-0.45
Akaline $*CO_2$	-0.47	-0.32	-0.16	-0.01	0.14	0.3	0.45	0.6	0.75
Neutral $*NO_3$	-3.21	-3.15	-3.09	-3.03	-2.98	-2.92	-2.86	-2.8	-2.74
Acid $*NO_3$	-7.46	-7.25	-7.04	-6.83	-6.62	-6.41	-6.19	-5.98	-5.77
Akaline $*NO_3$	-4.73	-4.84	-4.94	-5.04	-5.15	-5.25	-5.36	-5.46	-5.56

Refs:

1. S. D. Lacey, Q. Dong, Z. Huang, J. Luo, H. Xie, Z. Lin, D. J. Kirsch, V. Vattipalli, C. Povinelli, W. Fan, R. Shahbazian-Yassar, D. Wang, L. Hu, Nano Lett. 2019, 12, 5149.

2. H. Li, Y. Han, H. Zhao, W. Qi, D. Zhang, Y. Yu, W. Cai, S. Li, J. Lai, B. Huang, L. Wang, Nat. Commun. 2020, 11, 5437.

3. D. Zhang, Y. Shi, H. Zhao, W. Qi, X. Chen, T. Zhan, S. Li, B. Yang, M. Sun, J. Lai, B. Huang, L. Wang, J. Mater. Chem. A 2021, 2, 889.

4. D. Zhang, H. Zhao, X. Wu, Y. Deng, Z. Wang, Y. Han, H. Li, Y. Shi, X. Chen, S. Li, J. Lai, B. Huang, L. Wang, Adv. Funct. Mater. 2021, 31, 2006939.

5. Y. Chen, X. Zhan, S. L. A. Bueno, I. H. Shafei, H. M. Ashberry, K. Chatterjee, L. Xu, Y. Tang, S. E. Skrabalak, Nanoscale Horiz. 2021, 6, 231.

6. K. Huang, B. Zhang, J. Wu, T. Zhang, D. Peng, X. Cao, Z. Zhang, Z. Li, Y. Huang, J. Mater. Chem. A 2020, 8, 11938.

7. D. Wu, K. Kusada, T. Yamamoto, T. Toriyama, S. Matsumura, I. Gueye, O. Seo, J. Kim, S. Hiroi, O. Sakata, S. Kawaguchi, Y. Kubota, H. Kitagawa, Chem. Sci. 2020, 11, 12731.

8. D. Wu, K. Kusada, T. Yamamoto, T. Toriyama, S. Matsumura, S. Kawaguchi, Y. Kubota, H. Kitagawa, J. Am. Chem. Soc. 2020, 142, 13833.

9. K. V. Yusenko, S. Riva, P. A. Carvalho, M. V. Yusenko, S. Arnaboldi, A. S. Sukhikh, M. Hanfland, S. A. Gromilov, Scr. Mater. 2017, 138, 22.

10. M. W. Glasscott, A. D. Pendergast, S. Goines, A. R. Bishop, A. T. Hoang, C. Renault, J. E. Dick, Nat. Commun. 2019, 10, 2650.

11.S. Gao, S. Hao, Z. Huang, Y. Yuan, S. Han, L. Lei, X. Zhang, R. Shahbazian-Yassar, J. Lu, Nat. Commun. 2020, 11, 2016.

12. Z. Jin, J. Lv, H. Jia, W. Liu, H. Li, Z. Chen, X. Lin, G. Xie, X. Liu, S. Sun, H. J. Qiu, Small 2019, 15, 1904180. H.-J. Qiu, G. Fang, J. Gao, Y. Wen, J. Lv, H. Li, G. Xie, X. Liu, S. Sun, ACS Mater. Lett. 2019, 1, 526.

13. G. Fang, J. Gao, J. Lv, H. Jia, H. Li, W. Liu, G. Xie, Z. Chen, Y. Huang, Q. Yuan, X. Liu, X. Lin, S. Sun, H.-J. Qiu, Appl. Catal., B 2020, 268, 118431.

14. Y. Yao, Z. Huang, P. Xie, S. D. Lacey, R. J. Jacob, H. Xie, F. Chen, A. Nie, T. Pu, M. Rehwoldt, D. Yu, M. R. Zachariah, C. Wang, R. Shahbazian-Yassar, J. Li, L. Hu, Science 2018, 352, 1489.

15. R. Q. Yao, Y. T. Zhou, H. Shi, W. B. Wan, Q. H. Zhang, L. Gu, Y. F. Zhu, Z. Wen, X. Y. Lang, Q. Jiang, Adv. Funct. Mater. 2020, 31, 2009613.